

Assessing the nonlinear response of fine particles to precursor emissions: development and application of an Extended Response Surface Modeling technique (ERSM v1.0)

B. Zhao¹, S. X. Wang^{1,2}, K. Fu¹, J. Xing³, J. S. Fu⁴, C. Jang³, Y. Zhu⁵, X. Y. Dong⁴, Y. Gao^{4,6}, W. J. Wu¹, J. D. Wang¹, J. M. Hao^{1,2}

[1] State Key Joint Laboratory of Environment Simulation and Pollution Control, School of Environment, Tsinghua University, Beijing 100084, China

[2] State Environmental Protection Key Laboratory of Sources and Control of Air Pollution Complex, Beijing 100084, China

[3] U.S. Environmental Protection Agency, Research Triangle Park, North Carolina 27711, United States

[4] Department of Civil and Environmental Engineering, University of Tennessee, Knoxville, Tennessee 37996, United States

[5] School of Environmental Science and Engineering, South China University of Technology, Guangzhou 510006, China

[6] Atmospheric Science and Global Change Division, Pacific Northwest National Laboratory, Richland, Washington, 99352, United States

Correspondence to: S. X. Wang (shxwang@tsinghua.edu.cn)

Abstract.

An innovative Extended Response Surface Modeling technique (ERSM v1.0) is developed to characterize the nonlinear response of fine particles ($PM_{2.5}$) to large and simultaneous changes of multiple precursor emissions from multiple regions and sectors. The ERSM technique is developed starting from the conventional Response Surface Modeling (RSM) technique; it first quantifies the relationship between $PM_{2.5}$ concentrations and the emissions of gaseous precursors from each single region using the conventional RSM technique, and then assesses the effects of inter-regional transport of $PM_{2.5}$ and its gaseous precursors on $PM_{2.5}$ concentrations in the target region. We apply this novel technique with a widely used regional chemical transport model over the Yangtze River Delta (YRD) region of China, and evaluate

1 the response of $PM_{2.5}$ and its inorganic components to the emissions of 36
2 pollutant-region-sector combinations. The predicted $PM_{2.5}$ concentrations agree well with
3 independent chemical transport model simulations; the correlation coefficients are larger than
4 0.98 and 0.99, and the mean normalized errors are less than 1% and 2% for January and
5 August, respectively. It is also demonstrated that the ERSM technique could reproduce fairly
6 well the response of $PM_{2.5}$ to continuous changes of precursor emission levels between zero
7 and 150%. Employing this new technique, we identify the major sources contributing to $PM_{2.5}$
8 and its inorganic components in the YRD region. The nonlinearity in the response of $PM_{2.5}$ to
9 emission changes is characterized and the underlying chemical processes are illustrated.

11 **1 Introduction**

12 Fine particles (i.e., particulate matter less than or equal to $2.5 \mu m$ ($PM_{2.5}$)) worsen the
13 visibility (Zhang et al., 2012), pose serious health risks (Nel, 2005) and affect the Earth's
14 climate significantly (Stocker et al., 2013). For developing countries like China and India, the
15 attainment of stringent ambient $PM_{2.5}$ standards requires large reductions of both primary
16 particles and gaseous precursors (Wang and Hao, 2012). Cost-effective control policies need
17 to consider the impact of emission reductions of multiple pollutants from multiple regions and
18 sectors, and over a wide range of stringency levels. Therefore, it is strategically important to
19 assess the response of $PM_{2.5}$ to its precursor emissions from multiple sources, which is
20 typically nonlinear owing to complex chemical mechanisms.

21 Chemical Transport Models (CTMs) are the only viable tools for evaluating the response of
22 atmospheric concentrations to different control measures (Hakami et al., 2003). The most
23 widely used technique to evaluate these responses is sensitivity analysis, i.e., the computation
24 of derivatives of modeled concentrations with respect to emission rates. "Brute force" method
25 (Russell et al., 1995; Zhang et al., 2009b; Zhao et al., 2013c; Dong et al., 2014), the most
26 frequently used method for sensitivity analysis, involves one-at-a-time variable perturbation
27 and repeated solution of the model. It is straightforward but becomes inefficient for
28 decision-making when cost-effective emission controls need to optimize over various
29 pollutants from multiple sources. A number of mathematic techniques embedded in CTMs
30 have been developed to simultaneously calculate the sensitivities of the modeled
31 concentrations to multiple variables, including the Green Function Method (GFM) and its
32 variations (Hwang et al., 1978), Automatic Differentiation in FORtran (ADIFOR, Carmichael

1 et al., 1997), Direct Method (Dickerson et al., 1982), Decoupled Direct Method (DDM, Yang
2 et al., 1997), and Adjoint Sensitivity Analysis (Sandu et al., 2005; Hakami et al., 2006). These
3 methods are used for the calculation of first-order sensitivities, and are therefore not
4 applicable for large emission changes since the nonlinearity in atmospheric responses is not
5 captured by first-order sensitivities. Improved techniques incorporating second or
6 higher-order sensitivity analysis, e.g., High-order Decoupled Direct Method (HDDM, Hakami
7 et al., 2003), and Discrete Second Order Adjoint (Sandu and Zhang, 2008), are capable of
8 capturing the nonlinearity for a perturbation of the emissions of the base case. But as methods
9 for local sensitivity analysis, they are theoretically not reliable for predicting the response of
10 atmospheric concentrations to considerably large (e.g., >50-60%) emission reductions
11 (Yarwood et al., 2013), which are nevertheless very common in air quality policy-making of
12 developing countries like China (Zhao et al., 2013b; Wang et al., 2014). Recent studies
13 (Yarwood et al., 2013; Simon et al., 2013) tried to run HDDM at several emission levels and
14 use piecewise function to predict the atmospheric concentrations over a large emission range,
15 but this modified method is only suitable for 2-3 variables. More importantly, this group of
16 method could hardly predict the response of atmospheric concentrations when multiple (>3)
17 variables of precursor emissions change simultaneously.

18 Another group of methods involves building the relationship between the modeled
19 concentrations and emission rates using statistical techniques. This type of method is
20 applicable for various CTMs regardless of the chemical mechanisms, is user-friendly for
21 decision-makers, and is particularly suitable for assessing the atmospheric response to large
22 emission changes. Milford et al. (1989) and Fu et al. (2006) simulated the ozone
23 concentrations for a number of non-methane volatile organic compound (NMVOC) and NO_x
24 reduction combinations, and derived a set of “EKMA-like” (EKMA, Empirical Kinetics
25 Modeling Approach) control isopleths, but this method is only suitable for 2-3 variables.
26 Some other studies (Heyes et al., 1996; Wang and Milford, 2001; Amann et al., 2007)
27 empirically established analytic equations for the relationship between atmospheric
28 concentrations and emission rates, and determined the parameters based on relatively small
29 numbers of model simulations. However, Xing (2011) indicated that the nonlinearity in
30 atmospheric responses could not be captured in metropolitan regions unless fourth or higher
31 order equations were used, which restricted the feasibility and accuracy of analytic equations
32 (see details in the Supporting Information). The Response Surface Modeling (RSM) technique

1 (denoted by “conventional RSM” technique in the following text to distinguish from the
2 ERSM technique developed in this study), has been developed by using advanced statistical
3 techniques to characterize the relationship between model outputs and inputs. The number of
4 scenarios required to build RSM depends on the family of models chosen. Recently, the
5 conventional RSM technique has been applied to O₃ and PM_{2.5} related studies or
6 policy-making in the United States (U.S. Environmental Protection Agency, 2006a, b) and
7 China (Xing et al., 2011; Wang et al., 2011). In those applications, the relationships between
8 air pollutant concentrations and precursor emissions were established using the Maximum
9 Likelihood Estimation - Empirical Best Linear Unbiased Predictors (MLE-EBLUPs)
10 developed by Santner et al. (2003). Using this group of model, the number of model scenarios
11 required to build the RSM depends on the variable number via an equation of fourth or higher
12 order, even if the preferable sampling method and model configurations proposed by previous
13 studies (Santner et al., 2003) are used (see details in the Supporting Information). Therefore,
14 the required scenario number would be tens of thousands for over 15 variables and even
15 hundreds of thousands for over 25 variables, which is computationally impossible for most
16 three-dimensional CTMs. This proves a major limitation for the conventional RSM technique.
17 When considering the emissions of multiple pollutants from multiple sectors in multiple
18 regions, assessing the nonlinear response of PM_{2.5} to emission changes presents a big
19 challenge.

20 In response to this challenge, we developed a novel Extended Response Surface Modeling
21 technique (ERSM v1.0) in this study. Compared with the previous methods reviewed above,
22 this technique could characterize the nonlinear response of PM_{2.5} and its chemical
23 components to large and simultaneous changes of multiple precursor emissions from multiple
24 regions and sectors with a reasonable number of model scenarios. In particular, compared
25 with the conventional RSM technique, ERSM is applicable for an increased number of
26 variables and geographical regions. This technique is applied with the Community Multi-scale
27 Air Quality (CMAQ) model to evaluate the response of PM_{2.5} and its inorganic components to
28 precursor emissions over the Yangtze River Delta (YRD) region, one of the largest
29 city-clusters in China. The major sources contributing to PM_{2.5} and its inorganic components
30 in the YRD are identified and the nonlinearity in the response of PM_{2.5} to emission changes is
31 characterized.

1 **2 Methodology**

2 **2.1 Development of the ERSM Technique**

3 The ERSM technique is developed starting from the conventional RSM technique; the latter
4 characterizes the relationships between a response variable (e.g., $PM_{2.5}$ concentration) and a
5 set of control variables (i.e., emissions of particular precursors from particular sources)
6 following the procedures described in our previous paper (Xing et al., 2011). First, a number
7 of emission control scenarios are generated with the Latin Hypercube Sample (LHS) method
8 (Iman et al., 1980), a widely-used sampling method which ensures that the ensemble of
9 random samples is representative of actual variability. Then the $PM_{2.5}$ concentration for each
10 emission scenario is calculated with a regional CTM, and finally the RSM prediction system
11 is developed using a MPerK (MATLAB Parametric Empirical Kriging) program (Santner et
12 al., 2003) based on MLE-EBLUPs. The robustness of the conventional RSM technique has
13 been validated through leave-one-out cross validation, out of sample validation and 2-D
14 isopleths validation, as documented in our previous papers (Xing et al., 2011; Wang et al.,
15 2011).

16 The ERSM technique first quantifies the relationship between $PM_{2.5}$ concentrations and the
17 emissions of gaseous precursors from each single region with the conventional RSM
18 technique following the procedures described in the last paragraph, and then assesses the
19 effects of inter-regional transport of $PM_{2.5}$ and its gaseous precursors on $PM_{2.5}$ concentration
20 in the target region. In order to quantify the interaction among regions, we make a key
21 assumption that the emissions of gaseous precursors in the source region affect $PM_{2.5}$
22 concentrations in the target region through two major processes: (1) the inter-regional
23 transport of gaseous precursors enhancing the chemical formation of secondary $PM_{2.5}$ in the
24 target region; (2) the formation of secondary $PM_{2.5}$ in the source region followed by transport
25 to the target region. We quantify the contribution of these two processes to the interactions
26 between any two regions, and assess the inter-regional influences among multiple regions by
27 integrating the contributions of each process. Then, a particular approach was implemented to
28 improve the accuracy of the response surface when the gaseous emissions from multiple
29 regions experience quite large reductions simultaneously.

30 Finally, $PM_{2.5}$ concentrations are linearly dependent on primary $PM_{2.5}$ emissions, therefore we
31 predict the changes of $PM_{2.5}$ concentrations owing to the changes of primary $PM_{2.5}$ emissions

1 by simply interpolating between the base case and a sensitivity scenario where one control
2 variable of primary $PM_{2.5}$ is disturbed and the other variables stay constant.

3 Since the method to develop the relationship between $PM_{2.5}$ concentrations and primary $PM_{2.5}$
4 emissions is straightforward, we will focus on the response of $PM_{2.5}$ and its chemical species
5 to the emissions of gaseous precursors in the following texts. To facilitate the explanation, we
6 assume a simplified but general case which involves three regions, defined as A, B, and C,
7 and three control variables in each region, i.e., NO_x emissions of Sector 1, NO_x emissions of
8 Sector 2, and total NH_3 emissions. The response variable is $PM_{2.5}$ concentration in the urban
9 area of Region A. Although the technique is illustrated for this simplified case, it is also
10 applicable for different response variable (e.g., NO_3^- , SO_4^{2-} , and NH_4^+), and different numbers
11 of regions/pollutants/sectors. A detailed description of the ERSM technique using the
12 simplified case is given below, and a flowchart illustrating this technique is shown in Fig. 1.

13 The emission control scenarios required to construct ERSM include: (1) the base case; (2) N
14 scenarios generated by applying the LHS method for the control variables in each single
15 region; and (3) M scenarios generated by applying the LHS method for the total emissions of
16 gaseous precursors (NO_x and NH_3 for this case) in all regions. The scenario numbers N and
17 M are determined to ensure that they are sufficient to accurately construct the relationship
18 between the response variable and randomly changing control variables using conventional
19 RSM technique. Specifically, we gradually increase the scenario number and build the
20 conventional RSM repeatedly until the prediction performance is good enough based on the
21 results of out of sample validation (Xing et al., 2011; Wang et al., 2011). The mean
22 normalized error and correlation coefficients are selected as indices of prediction performance.

23 In our previous paper (Xing et al., 2011), we showed that the normalized mean error first
24 decreases and then gradually remains stable, with the increase of scenario number. In contrast,
25 the correlation coefficient first increases and then gradually becomes stable. We used a
26 criterion that mean normalized error $< 1\%$ and correlation coefficient > 0.99 , and determined
27 that 30 and 50 scenarios were required to construct the conventional RSM for 2 and 3
28 variables, respectively. Therefore, for the simplified case, $N=50$, and $M=30$. The required
29 scenario number for the simplified case is therefore 1 (the base case) $+ 50$ (scenarios for each
30 single region) $* 3$ (number of regions) $+ 30$ (scenarios for the total precursor emissions in all
31 regions) $= 181$.

1 Employing conventional RSM technique, we build the response surface of PM_{2.5}
 2 concentration in Region A to the concentrations of precursors in Region A using the base case
 3 and the 50 scenarios where the variables in Region A change randomly but those in other
 4 regions remain constant:

$$5 \quad [PM_{2.5}]_A = [PM_{2.5}]_{A0} + RSM_{A \rightarrow A}^{PM_{2.5}}([NOx]_A, [NH3]_A) \quad (1)$$

6 where $[PM_{2.5}]_A$, $[NOx]_A$, and $[NH3]_A$ are the concentrations of PM_{2.5}, NO_x and NH₃ in
 7 Region A, respectively. $[PM_{2.5}]_{A0}$ is the PM_{2.5} concentration in Region A in the base case.
 8 *RSM* represents the response surface we build with conventional RSM technique; the
 9 superscript (“PM_{2.5}” in this case) represents the response variable; the letters before and after
 10 the arrow in the subscript (both are “A” in this case) represent the source and receptor regions,
 11 respectively. Further, we develop the relationship between precursor concentrations and the
 12 changes of precursor emissions in Region A with the same 51 scenarios (we use NO_x
 13 concentration as example, and it is equivalent for NH₃):

$$14 \quad [NOx]_{A \rightarrow A} = RSM_{A \rightarrow A}^{NOx}(Emis_NOx_1_A, Emis_NOx_2_A, Emis_NH3_A) \quad (2)$$

15 where $Emis_NOx_1_A$, $Emis_NOx_2_A$, and $Emis_NH3_A$ are NO_x emissions of Sector 1, NO_x
 16 emissions of Sector 2, and total NH₃ emissions in Region A, respectively. $[NOx]_{A \rightarrow A}$,
 17 representing the changes of NO_x concentration in Region A compared with the base case in
 18 response to the emission changes in the same region, is defined as

$$19 \quad [NOx]_{A \rightarrow A} = [NOx]_A - [NOx]_{A0} \quad (3)$$

20 where $[NOx]_{A0}$ is the NO_x concentration in Region A in the base case.

21 Following similar procedures, the response of the concentrations of PM_{2.5} and its gaseous
 22 precursors in Region A to the changes of precursor emissions in Region B (the same method
 23 applies for Region C) can be developed using the base case and the 50 scenarios where the
 24 variables in Region B change randomly but those in other regions remain constant:

$$25 \quad [PM_{2.5}]_{B \rightarrow A} = RSM_{B \rightarrow A}^{PM_{2.5}}(Emis_NOx_1_B, Emis_NOx_2_B, Emis_NH3_B) \quad (4)$$

$$26 \quad [NOx]_{B \rightarrow A} = RSM_{B \rightarrow A}^{NOx}(Emis_NOx_1_B, Emis_NOx_2_B, Emis_NH3_B) \quad (5)$$

$$27 \quad [NH3]_{B \rightarrow A} = RSM_{B \rightarrow A}^{NH3}(Emis_NOx_1_B, Emis_NOx_2_B, Emis_NH3_B) \quad (6)$$

28 where $[PM_{2.5}]_{B \rightarrow A}$, $[NOx]_{B \rightarrow A}$, and $[NH3]_{B \rightarrow A}$ are the changes of PM_{2.5}, NO_x, and NH₃
 29 concentrations in Region A compared with the base case in response to the emission changes
 30 in Region B. $Emis_NOx_1_B$, $Emis_NOx_2_B$, and $Emis_NH3_B$ are NO_x emissions of Sector
 31 1, NO_x emissions of Sector 2, and total NH₃ emissions in Region B, respectively.

1 As described above, the influence of gaseous precursor emissions in Region B on PM_{2.5}
2 concentration in Region A, as expressed by Eq. (4), can be broken down into two major
3 processes: (1) the transport of gaseous precursors from Region B to Region A that enhances
4 the chemical formation of secondary PM_{2.5} in Region A; (2) the formation of secondary PM_{2.5}
5 in Region B followed by transport to Region A. In order to quantify the contribution of the
6 first process, we firstly use Eq. (5) and Eq. (6) to quantify the effect of the transport of
7 gaseous precursors from Region B to Region A on the precursor concentrations in Region A.
8 How much does the change of precursor concentrations in Region A enhance the chemical
9 formation of secondary PM_{2.5} in Region A? To answer this question, we introduce a
10 straightforward assumption that the changes of PM_{2.5} concentration owing to changes of
11 precursor concentrations in the same region (described by Eq. (1)) are solely attributable to
12 changes of local chemical formation. Strictly speaking, the changes of precursor concentration
13 in Region A might affect the precursor concentrations/PM_{2.5} concentrations in other regions,
14 which might in turn affect the PM_{2.5} concentrations in Region A; but this “indirect” pathway
15 is neglected in this study. For the case study over the YRD region (see details of the case
16 study in Sect. 2.2), we estimate that, when the concentrations of NO_x, SO₂, and NH₃ in a
17 specific region (Shanghai, Jiangsu, or Zhejiang) are all reduced 50%, the “indirect” pathway
18 could only account for less than 2% of the total PM_{2.5} reduction (see details in the Supporting
19 Information). This confirms our assumption that the “indirect” pathway is negligible.

20 Based on this assumption, the contribution of the first process to PM_{2.5} concentrations in
21 Region A is expressed as

$$22 \quad [PM_{2.5-}Chem]_{B \rightarrow A} = RSM_{A \rightarrow A}^{PM_{2.5}} ([NO_x]_{A0} + [NO_x]_{B \rightarrow A}, [NH_3]_{A0} + [NH_3]_{B \rightarrow A}) \quad (7)$$

23 where $[PM_{2.5-}Chem]_{B \rightarrow A}$ is the change of PM_{2.5} concentration in Region A affected by the
24 changes of precursor emissions in Region B through the inter-regional transport of gaseous
25 precursors (the first process). The contribution of the second process to PM_{2.5} concentration in
26 Region A (denoted by $[PM_{2.5-}Trans]_{B \rightarrow A}$ defined below) is then calculated by extracting the
27 contribution of the first process (Eq. (7)) from the total (Eq. (4)), as expressed by Eq. (8).

$$28 \quad [PM_{2.5-}Trans]_{B \rightarrow A} = [PM_{2.5}]_{B \rightarrow A} - [PM_{2.5-}Chem]_{B \rightarrow A} \quad (8)$$

29 where $[PM_{2.5-}Trans]_{B \rightarrow A}$ is the change of PM_{2.5} concentration in Region A affected by the
30 changes of precursor emissions in Region B through the transport of secondary PM_{2.5} (the
31 second process).

1 We also need to know the relationship between $[PM_{2.5-Trans}]_{B \rightarrow A}$ and the precursor
 2 emissions in Region B. Therefore, we quantify this relationship using conventional RSM
 3 technique, as described by Eq. (9).

$$4 \quad [PM_{2.5-Trans}]_{B \rightarrow A} = RSM_{B \rightarrow A}^{PM_{2.5-Trans}}(Emis_NOx_1_B, Emis_NOx_2_B, Emis_NH3_B) \quad (9)$$

5 For the emission scenario whose $PM_{2.5}$ concentration is to be predicted, we presume that its
 6 emissions of gaseous precursors in all the three regions are arbitrary. In this case, the change
 7 of $PM_{2.5}$ is expressed as an integrated effect of the changes of local precursor emissions, the
 8 inter-regional transport of precursors enhancing local chemical reactions, and the
 9 inter-regional transport of secondary $PM_{2.5}$:

$$10 \quad [PM_{2.5}]_A = [PM_{2.5}]_{A0} + RSM_{A \rightarrow A}^{PM_{2.5}}([NOx]_{A0} + [NOx]_{A \rightarrow A} + [NOx]_{B \rightarrow A} + [NOx]_{C \rightarrow A}, \\ 11 \quad [NH3]_{A0} + [NH3]_{A \rightarrow A} + [NH3]_{B \rightarrow A} + [NH3]_{C \rightarrow A}) + [PM_{2.5-Trans}]_{B \rightarrow A} + [PM_{2.5-Trans}]_{C \rightarrow A} \quad (10)$$

12 where $[PM_{2.5-Trans}]_{B \rightarrow A}$ is calculated using Eq. (9), and $[PM_{2.5-Trans}]_{C \rightarrow A}$ is calculated
 13 using an equivalent equation for which the independent variables are the gaseous emissions in
 14 Region C. It should be noted that $[PM_{2.5-Trans}]_{B \rightarrow A}$ cannot be calculated using Eq. (8)
 15 because Eq. (8) holds only if the emissions in the regions other than Region B remain at the
 16 base-case levels.

17 Strictly speaking, $[PM_{2.5-Trans}]_{B \rightarrow A}$ and $[PM_{2.5-Trans}]_{C \rightarrow A}$ could interact with each other.
 18 In other words, the changes of precursor emissions in Region C might affect the formation of
 19 secondary $PM_{2.5}$ in Region B, which further affects the transport of secondary $PM_{2.5}$ from
 20 Region B to Region A. Eq. (9) and Eq. (10) implies an assumption that $[PM_{2.5-Trans}]_{B \rightarrow A}$
 21 depends only on the precursor emissions in Region B, and is independent of precursor
 22 emissions in other regions. That is, the interaction between $[PM_{2.5-Trans}]_{B \rightarrow A}$ and
 23 $[PM_{2.5-Trans}]_{C \rightarrow A}$ is neglected. For the case study over the YRD region, we estimate that,
 24 the reduction of precursor emissions in Jiangsu and Others by 50% could only change
 25 $[PM_{2.5-Trans}]_{Zhejiang \rightarrow Shanghai}$ (i.e., the change of $PM_{2.5}$ concentration in Shanghai affected by
 26 the changes of precursor emissions in Zhejiang through the transport of secondary $PM_{2.5}$) by
 27 less than 1% (see details in the Supporting Information). This confirms the above-mentioned
 28 assumption.

29 It should be noted that Eq. (1), which relates the changes of $PM_{2.5}$ concentration in Region A
 30 (equivalent to the changes of local chemical formation of $PM_{2.5}$ as discussed above) to local
 31 precursor concentrations, is established using the base case and the 50 scenarios where the
 32 variables in Region A change randomly but those in other regions remain constant. This

1 means Eq. (1) is only applicable for the concentration range below (we use NO_x as example,
 2 it is equivalent for NH₃)

$$3 \quad [NOx]_A \geq [NOx]_{A, min} = [NOx]_{A0} + [NOx]_{A \rightarrow A, min} = [NOx]_{A0} + RSM_{A \rightarrow A}^{NOx}(0, 0, 0) \quad (11)$$

4 where $[NOx]_{A, min}$ is defined as the minimum NO_x concentration in Region A when the
 5 emissions from Region A change arbitrarily and those in other regions remain the base-case
 6 levels.

7 Eq. (10) relies on Eq. (1) but might exceed its available range, i.e., $[NOx]_A < [NOx]_{A, min}$, or
 8 $[NH3]_A < [NH3]_{A, min}$, when the precursor emissions in multiple regions are reduced
 9 considerably at the same time. In this case, we quantify the changes of PM_{2.5} concentrations
 10 owing to local chemical formation through a different approach. First, the local chemical
 11 formation of PM_{2.5} can be tracked easily in widely-used three-dimensional CTMs. For
 12 example, a module named “process analysis” has already been implemented in CMAQ, which
 13 outputs the contribution of major physical and chemical processes to air pollutant
 14 concentrations. The chemical formation of PM_{2.5} in Region A is estimated as

$$15 \quad Prod_PM_A = AERO_PM_A + CLDS_PM_A \quad (12)$$

16 where $AERO_PM_A$ and $CLDS_PM_A$ are the contribution of aerosol process and in-cloud
 17 process to PM_{2.5} concentration in Region A, extracted from CMAQ using the module
 18 “process analysis”. When the ERSM technique is applied with other CTMs, the chemical
 19 formation of PM_{2.5} can be readily extracted in a similar way. In addition, the chemical
 20 formation of PM_{2.5} in Region A and the resulting PM_{2.5} concentrations present a linear
 21 relationship, which can be established using the base case and the 50 scenarios where the
 22 variables in Region A change randomly but those in other regions remain constant:

$$23 \quad [PM_{2.5}]_A = k \cdot Prod_PM_A + b \quad (13)$$

24 where k and b are parameters determined through regression, and the correlation coefficient
 25 is approximately 0.99. Then we develop the relationship between the local chemical
 26 formation of PM_{2.5} in Region A and local precursor concentrations using the base case and the
 27 30 scenarios where control variables in all regions change together and the variables for the
 28 same pollutant (e.g., $Emis_NH3_A$, $Emis_NH3_B$, and $Emis_NH3_C$) equal each other:

$$29 \quad Prod_PM_A = RSM_{A \rightarrow A}^{Prod_PM}([NOx]_A, [NH3]_A) \quad (14)$$

30 Combining Eq. (13) and Eq. (14), and considering the effect of inter-regional transport of
 31 PM_{2.5} (calculated using Eq. (9)), we derive

$$[PM_{2.5}]_A = k \cdot RSM_{A \rightarrow A}^{Prod_PM} ([NOx]_{A0} + [NOx]_{A \rightarrow A} + [NOx]_{B \rightarrow A} + [NOx]_{C \rightarrow A},$$

$$1 \quad [NH3]_{A0} + [NH3]_{A \rightarrow A} + [NH3]_{B \rightarrow A} + [NH3]_{C \rightarrow A}) + b + [PM_{2.5_Trans}]_{B \rightarrow A} + [PM_{2.5_Trans}]_{C \rightarrow A}$$

$$2 \quad (\text{applicable for } [NOx]_A < [NOx]_{A, min}, \text{ or } [NH3]_A < [NH3]_{A, min}) \quad (15)$$

3 It should be noted that the “process analysis” module could also be used within the first
4 approach (Eq. (10)) to distinguish the contributions of chemical formation and physical
5 transport. However, in the first approach, we could distinguish the chemical and transport
6 contributions even without this diagnostic module (see Eq. (7) and Eq. (8)). If this module
7 was used, we would need to develop the relationship between the chemically formed $PM_{2.5}$
8 and the $PM_{2.5}$ concentration, which was an extra step compared with the first approach and
9 added to the complexity.

10 To assure the consistency between Eq. (10) and Eq. (15), we introduce “transition intervals”
11 of $([NOx]_{A, min}, [NOx]_{A, min} + \delta_{NOx})$ and $([NH3]_{A, min}, [NH3]_{A, min} + \delta_{NH3})$, where
12 $\delta_{NOx} = 0.1 * [NOx]_{A0}$ and $\delta_{NH3} = 0.1 * [NH3]_{A0}$. Eq. (10) is applied for
13 $[NOx]_A \geq [NOx]_{A, min} + \delta_{NOx}$ and $[NH3]_A \geq [NH3]_{A, min} + \delta_{NH3}$, and we linearly interpolate
14 between Eq. (10) and Eq. (15) for the transitional range. Based on the case study in the YRD
15 region (see Sect. 2.2), the discrepancy between the two approaches is 1-8% in the transition
16 interval.

17 **2.2 Case study of the YRD region**

18 The ERSM technique was applied with CMAQ version 4.7.1 over the YRD region of China.
19 One-way, triple nesting simulation domains are used, as shown in Fig. 2. Domain 1 covers
20 most of China and part of East Asia with a grid resolution of 36 km×36 km; domain 2 covers
21 the eastern China with a grid resolution of 12 km×12 km; domain 3 covers the Yangtze River
22 Delta region with a grid resolution of 4 km×4 km. The Weather Research and Forecasting
23 Model (WRF, version 3.3) was used to generate the meteorological fields. The physical and
24 chemical options of CMAQ and WRF, the geographical projection, the vertical resolution,
25 and the initial and boundary conditions are consistent with our previous papers (Zhao et al.,
26 2013a, c). A high-resolution anthropogenic emission inventory for the YRD region developed
27 by Fu et al. (2013) was used. The anthropogenic emissions for other regions in East Asia were
28 from Zhao et al. (2013a, c) and Wang et al., (2014), and emissions for other Asian countries
29 were taken from the INDEX-B inventory (Zhang et al., 2009a). The biogenic emissions were
30 calculated by the Model of Emissions of Gases and Aerosols from Nature (MEGAN,

1 Guenther et al., 2006). The ERSM technique is applicable for various time scales, ranging
2 from a single day to several years. The simulation period for this case study is January and
3 August in 2010, representing winter and summer, respectively. One may want to extend the
4 analysis to a full year. The most rigorous way is to finish the CMAQ simulations for a full
5 year and build the response surfaces following the same procedure. Alternatively, the
6 relationship for a full year can be roughly estimated using the average values of January and
7 August. Another approach is to finish the simulations for an additional month in Spring and
8 Autumn, respectively, and represent the situation of a full year with the average values of the
9 four typical months. The simulated meteorological parameters, and concentrations of PM₁₀,
10 PM_{2.5}, and their chemical components agree fairly well with observation data, as described in
11 detail in the Supporting Information (Table S3-S4, Fig. S3-S5).

12 Domain 3 was divided into 4 regions (see Fig. 2), i.e. Shanghai, southern Jiangsu province
13 (“Jiangsu”), northern Zhejiang province (“Zhejiang”), and other regions (“Others”). We
14 developed two RSM/ERSM prediction systems (Table 1); the response variables for both of
15 them are the concentrations of PM_{2.5}, SO₄²⁻, and NO₃⁻ over the urban areas of major cities (see
16 Fig. 2) in these four regions. The first prediction system used the conventional RSM
17 technique and 101 emission control scenarios generated by the LHS method to map
18 atmospheric concentrations versus total emissions of NO_x, SO₂, NH₃, NMVOC, and PM_{2.5} in
19 Domain 3. For the second prediction system, the emissions of gaseous PM_{2.5} precursors and
20 primary PM_{2.5} in each of the four regions are categorized into 6 and 3 control variables,
21 respectively (see Table 1), resulting in 36 control variables in total. Note that we did not
22 consider NMVOC emissions in the second prediction system, because the contribution of
23 NMVOC to PM_{2.5} concentrations is small in the current CMAQ model, mainly due to the
24 significant underestimation of secondary organic aerosol formation (Carlton et al., 2010). We
25 generated 663 scenarios (see Table 1) to build the response surface, following the method to
26 create emission scenarios for the ERSM technique (the 5th paragraph of Sect. 2.1). In detail,
27 the scenarios include (1) 1 CMAQ base case; (2) N=150 scenarios generated by applying LHS
28 method for the control variables of gaseous precursors in Shanghai, 150 scenarios generated
29 in the same way for Jiangsu, 150 scenarios for Zhejiang, and 150 scenarios for Others; (3)
30 M=50 scenarios generated by applying LHS method for the total emissions of NO_x, SO₂, and
31 NH₃ in all regions; and (4) 12 scenarios where one of the control variables of primary PM_{2.5}
32 emissions is set to 0.25 for each scenario. Here the number N=150 and M=50 are determined

1 according to the numerical experiments conducted in our previous studies (Xing et al., 2011;
2 Wang et al., 2011), which showed that the response surface for 6 and 3 variables could be
3 built with good prediction performance (mean normalized error < 1%; correlation coefficient >
4 0.99) using 150 and 50 scenarios, respectively. Finally, we generated 40 independent
5 scenarios for out-of-sample validation, as described in detail in Sect. 3.1.

6 **3 Results and discussion**

7 **3.1 Validation of ERSM performance**

8 The performance of the conventional RSM technique has been well evaluated in our previous
9 studies (Xing et al., 2011; Wang et al., 2011). In this study we focus on the validation of the
10 ERSM technique. Using the prediction system built with the ERSM technique, we predicted
11 the PM_{2.5} concentrations for 40 “out-of-sample” control scenarios, i.e., scenarios independent
12 from those used to build the ERSM prediction system, and compared with the corresponding
13 CMAQ simulations. These 40 out-of-sample scenarios include 32 cases (case 1-32) where the
14 control variables of gaseous precursors change but those of primary PM_{2.5} stay the same as
15 the base case, 4 cases (case 33-36) the other way around, and 4 cases (case 37-40) where
16 control variables of gaseous precursors and primary PM_{2.5} change simultaneously. Most cases
17 are generated randomly with the LHS method (case 4-6, 10-12, 16-18, 22-24, 28-40), and
18 some cases are designed where all control variables are subject to large emission changes
19 (case 1-3, 7-9, 13-15, 19-21, 25-27). A more detailed description of the out-of-sample control
20 scenarios is given in Table S5. Two statistical indices, the Normalized Error (NE) and Mean
21 Normalized Error (MNE) are defined as follows:

$$22 \text{ NE} = |P_i - S_i| / S_i \quad (16)$$

$$23 \text{ MNE} = \frac{1}{N_s} \sum_{i=1}^{N_s} [|P_i - S_i| / S_i] \quad (17)$$

24 where P_i and S_i are the ERSM-predicted and CMAQ-simulated value of the i^{th}
25 out-of-sample scenario; N_s is the number of out-of-sample scenarios. Figure 3 compares the
26 ERSM-predicted and CMAQ-simulated PM_{2.5} concentrations for the out-of-sample scenarios
27 using scattering plots (the raw data for the scattering plots are given in Table S6-S7). Table 2
28 shows the statistical results for the comparison. It can be seen that the ERSM predictions and
29 CMAQ simulations agree well with each other. The correlation coefficients are larger than
30 0.98 and 0.99, and the MNEs are less than 1% and 2% for January and August, respectively.
31 The maximum NEs could be as large as 6% and 10% in January and August, respectively, but

1 the NEs for 95% of all out-of-sample scenarios fall below 3.5%. NEs exceeding 3.5% happen
2 only for the scenario where all control variables are reduced by 90% (case 25). In addition,
3 the maximum NEs for case 33-36 are all within 0.2%, indicating a perfect linear relationship
4 between PM_{2.5} concentrations and primary PM_{2.5} emissions.

5 We further evaluated the performance of the ERSM technique by comparing the 2D-isopleths
6 of PM_{2.5} concentrations in response to the simultaneous changes of NO_x/SO₂/NH₃ emissions
7 in all regions derived from both the conventional RSM and the ERSM technique. Figure 4, S6,
8 and S7 show the isopleths of PM_{2.5} concentrations in Shanghai, Jiangsu, and Zhejiang,
9 respectively. The X- and Y-axis of the figures show the “emission ratio”, defined as the ratios
10 of the changed emissions to the emissions in the base case. For example, an emission ratio of
11 1.5 means the emissions of a particular control variable increase by 50% from the base case.
12 The different colors represent different PM_{2.5} concentrations. The comparison shows that the
13 shapes of isopleths derived from both prediction systems agree fairly well with each other,
14 although the isopleths predicted by the ERSM technique are not as smooth as those predicted
15 by the conventional RSM technique owing to a much larger variable number. The consistency
16 between the conventional RSM and ERSM prediction systems indicates that the ERSM
17 technique could reproduce fairly well the response of PM_{2.5} to continuous changes of
18 precursor emission levels between zero and 150%. Although model simulations definitely
19 have numerical errors, the success in capturing the atmospheric responses to continuous
20 emission changes over a full range of control levels ensures that these errors could not
21 challenge the major conclusions about the effectiveness of air pollution control measures.

22 **3.2 Response of PM_{2.5} to precursor emissions.**

23 The ERSM prediction system could instantly evaluate the response of PM_{2.5} and its chemical
24 components to the independent or simultaneous changes of the precursor emissions from
25 multiple sectors and regions, over a full range of control levels. Therefore, it improves the
26 identification of major precursors, regions, and sectors contributing to PM_{2.5} pollution. This
27 unique capability distinguishes the ERSM from the previous sensitivity analysis methods.

28 Following previous sensitivity studies, we define PM_{2.5} sensitivity as the change ratio of
29 PM_{2.5} concentration divided by the reduction ratio of emissions:

$$30 S_a^X = [(C^* - C_a) / C^*] / (1 - a) \quad (18)$$

31 where S_a^X is the PM_{2.5} sensitivity to emission source X at its emission ratio a ; C_a is the
32 concentration of PM_{2.5} when the emission ratio of X is a ; and C^* is the concentration of

1 $PM_{2.5}$ in the base case (when emission ratio of X is 1). Figure 5 shows the $PM_{2.5}$ sensitivity to
2 the stepped control of individual air pollutants, and Fig. 6 shows the $PM_{2.5}$ sensitivity to the
3 stepped control of individual air pollutants from individual sectors. Figure 5 can be derived
4 from the prediction systems built with both the conventional RSM and ERSM technique,
5 except that the latter did not evaluate the effects of the changes of NMVOC emissions. The
6 results derived from both systems are consistent, and we present those derived from the
7 conventional technique to include the effects of NMVOC. Figure 6 is derived from the ERSM
8 technique.

9 In January, $PM_{2.5}$ concentrations are sensitive to the primary $PM_{2.5}$ emissions, followed by
10 NH_3 , and relatively insensitive to NO_x and SO_2 . The contribution of primary $PM_{2.5}$ is
11 dominated by the emissions from industrial and residential sources. During August, gaseous
12 precursors make larger contributions to $PM_{2.5}$ concentrations than primary $PM_{2.5}$, with similar
13 contributions from NH_3 , SO_2 , and NO_x . The NO_x emissions from power plants, the industrial
14 and residential sector, and the transportation sector play similar roles; the SO_2 emissions from
15 the industrial and residential sector have larger effects on $PM_{2.5}$ than those from power plants
16 due to larger emissions and lower stack heights. NMVOC emissions have minor effect on
17 $PM_{2.5}$ concentrations, mainly due to the significant underestimation of SOA in the current
18 version of CMAQ, which is also a common issue for most widely used CTMs (Robinson et al.,
19 2007).

20 The $PM_{2.5}$ sensitivities to primary $PM_{2.5}$ emissions are approximately the same at various
21 control levels. However, the $PM_{2.5}$ sensitivity to gaseous precursors increases notably when
22 more control efforts are taken, mainly attributable to transition between NH_3 -rich and
23 NH_3 -poor conditions. Specifically, a particular pollutant (SO_2 , NO_x , or NH_3), when subject to
24 larger reductions compared with others, will become the limiting factor for inorganic aerosol
25 chemistry. In January, the response of $PM_{2.5}$ to NO_x emissions is negative for relatively small
26 reductions (< 40-70%), but becomes positive for large reductions (> 40-70%). This strong
27 nonlinearity has also been confirmed by the previous studies (Zhao et al., 2013c; Dong et al.,
28 2014). Relatively small reductions of NO_x emissions lead to the increase of O_3 and HO_x
29 radical due to a NMVOC-limited regime for photochemistry, enhancing the formation of
30 sulfate (see Fig. 7). In addition, the increase of O_3 and HO_x radical also accelerates the
31 nighttime formation of N_2O_5 and HNO_3 through the $NO_2 + O_3$ reaction, thereby enhancing the
32 formation of nitrate aerosol (see Fig. 7). As an integrated effect, the $PM_{2.5}$ concentrations

1 increase with relatively small reductions of NO_x emissions. Under large reductions of NO_x ,
2 $\text{PM}_{2.5}$ concentrations decrease, resulting from the simultaneous decline of NO_2 , O_3 and HO_x
3 radical concentrations (NO_x -limited regime for photochemistry). These chemical processes
4 also explain why the reduction of NO_x emissions of a single emission sector has negative
5 effects on $\text{PM}_{2.5}$ even at large reduction ratio (see Fig. 6). Simultaneous reductions of NO_x
6 emissions from multiple sectors are essential for reducing $\text{PM}_{2.5}$ concentrations. If all
7 pollutants are controlled simultaneously, the sensitivity of $\text{PM}_{2.5}$ concentrations to emission
8 reductions also generally becomes larger with more control effort taken, especially in January
9 (see red dotted line in Fig. 5 and Fig. 6). Note that the effects of reducing individual pollutants
10 (from individual sectors) and reducing all of them together are different. In most cases the
11 combined effect is lower than the sum of individual effects, which can be explained by the
12 overlap effects of reductions in both species involved in the formation of ammonium sulfate
13 and ammonium nitrate. However, it is sometimes the other way around in January, as shown
14 in Fig. 6. As mentioned above, in January, the response of $\text{PM}_{2.5}$ to the reduction of NO_x
15 emissions from a single emission sector is negative since the emission reduction is small
16 compared with the total NO_x emissions. Therefore, when the NO_x emissions from each sector
17 are reduced individually (the bars), we sum up the negative effects. In contrast, when all
18 pollutants from all sectors are reduced simultaneously (the red dotted line), the NO_x emission
19 reduction at large ratio could have positive effect on $\text{PM}_{2.5}$ reduction. This is why the
20 combined effect sometimes exceeds the sum of individual effects in January.

21 Then, we evaluate the contribution of primary $\text{PM}_{2.5}$ and gaseous precursor (SO_2 , NO_x , and
22 NH_3) emissions from different regions to $\text{PM}_{2.5}$ concentrations based on the ERSM technique
23 (Table 3). The contributions of total primary $\text{PM}_{2.5}$ emissions (39-46% in January, and 43-46%
24 in August) are dominated by local sources (32-36% in January, and 37-43% in August). Total
25 gaseous precursor emissions in the domain contribute 25-36% and 48-50% of $\text{PM}_{2.5}$
26 concentrations in January and August, respectively. The relative importance of gaseous
27 precursor emissions from the other regions compared with local precursor emissions is
28 generally higher than that of primary $\text{PM}_{2.5}$; this trend is especially evident in August. In
29 Shanghai, the gaseous precursor emissions from Jiangsu and Zhejiang even contribute more
30 to the $\text{PM}_{2.5}$ concentration than local precursor emissions during August. In January, long
31 range transport has a significant effect on $\text{PM}_{2.5}$ concentrations (25-34% contribution) due to
32 the northerly monsoon, contrasted by the minor effect in August (7-8% contribution).

1 **3.3 Response of SO_4^{2-} and NO_3^- to precursor emissions**

2 We pay special attention to secondary inorganic aerosols (SIA) because SIA contribute 28-55%
3 of total $\text{PM}_{2.5}$ concentrations based on our simulation. Figure 7 shows the sensitivity of
4 $\text{NO}_3^-/\text{SO}_4^{2-}$ concentrations to the emissions of individual air pollutants in individual regions;
5 Fig. S8 shows the sensitivity of $\text{NO}_3^-/\text{SO}_4^{2-}$ concentrations to the emissions of individual air
6 pollutants from individual sectors. Both figures are derived from the prediction system built
7 with the ERSM technique. In January, NO_3^- concentration is most sensitive to NH_3 emissions,
8 especially local NH_3 emissions. The effect of local NO_x emissions on NO_3^- concentrations
9 changes from negative to positive when the controls of NO_x emissions become more and
10 more stringent. This pattern is similar to that of $\text{PM}_{2.5}$ described above. The NO_x emissions
11 from the industrial and residential sector and the transportation sector, when controlled
12 individually, both make negative contribution to the reduction of NO_3^- concentrations. In
13 contrast, the control of NO_x emissions from power plants often favors the reduction of NO_3^- ,
14 because power plants tend to affect the fine particles over a larger spatial scale due to their
15 higher release heights, and because the photochemistry typically changes from a
16 NMVOC-limited regime in surface metropolis areas to a NO_x -limited regime in vast rural
17 areas or the upper air (Xing et al., 2011). In August, NO_3^- concentrations are mainly affected
18 by local emissions of NH_3 and NO_x , as well as NO_x emissions in upwind regions, and NO_x
19 emissions make a much larger positive contribution to NO_3^- concentrations compared with
20 January. Factors accounting for this difference include a stronger NH_3 -rich condition for
21 inorganic aerosol chemistry (Wang et al., 2011), and a weaker NMVOC-limited (in
22 metropolis areas) or a stronger NO_x -limited (in rural areas) photochemical condition in
23 August. The contributions of NO_x emissions from power plants, the industrial and residential
24 sector, and the transportation sector are similar to each other.

25 In January, SO_4^{2-} concentrations are dominated by the changes of local SO_2 emissions,
26 followed by local NH_3 emissions. NO_x emissions have a negative effect on SO_4^{2-} due to both
27 thermodynamic (competition with SO_2 for NH_3) and photochemical effect (negatively
28 correlated with O_3 and HO_x radical). In August, SO_4^{2-} is most sensitive to local SO_2 and NH_3
29 emissions. In Shanghai, where local emissions are relatively small compared with emissions
30 in other regions, the SO_2 and NH_3 emissions from upwind regions might contribute more to
31 SO_4^{2-} concentration than local emissions. In both January and August, the SO_2 emissions of

1 the industrial and residential sector have larger effects on SO_4^{2-} concentrations than those of
2 power plants, partly due to larger emissions and lower stack heights.

3 **4 Conclusions, implications, and limitations**

4 In this study, we developed a novel Extended Response Surface Modeling technique (ERSM
5 v1.0). As an advantage over previous models or techniques, this technique could
6 characterize the nonlinear response of $\text{PM}_{2.5}$ and its chemical components to large and
7 simultaneous changes of multiple precursor emissions from multiple regions and sectors with
8 a reasonable number of model scenarios. The ERSM technique was developed starting from
9 the conventional RSM technique; it first quantifies the relationship between $\text{PM}_{2.5}$
10 concentrations and the emissions of gaseous precursors from each single region with the
11 conventional RSM technique, and then assesses the effects of inter-regional transport of $\text{PM}_{2.5}$
12 and its gaseous precursors on $\text{PM}_{2.5}$ concentrations in the target region. A particular approach
13 was implemented to improve the accuracy of the response surface when the emissions from
14 multiple regions experience quite large reductions simultaneously.

15 We applied the ERSM technique with CMAQ version 4.7.1 over the YRD region of China,
16 and mapped the concentrations of $\text{PM}_{2.5}$ and its inorganic components versus 36 control
17 variables. Using the ERSM technique, we predicted the $\text{PM}_{2.5}$ concentrations for 40
18 independent control scenarios, and compared with the corresponding CMAQ simulations. The
19 comparison results show that the ERSM predictions and CMAQ simulations agree well with
20 each other. The correlation coefficients are larger than 0.98 and 0.99, and the mean
21 normalized errors are less than 1% and 2% for January and August, respectively. We also
22 compared the 2D-isopleths of $\text{PM}_{2.5}$ concentrations in response to the changes of precursor
23 emissions derived from both the conventional RSM and the ERSM technique, and
24 demonstrated that the ERSM technique could reproduce fairly well the response of $\text{PM}_{2.5}$ to
25 continuous changes of precursor emission levels between zero and 150%.

26 Employing the ERSM technique, we identified the major sources contributing to $\text{PM}_{2.5}$ and its
27 inorganic components in the YRD region. For example, in January, $\text{PM}_{2.5}$ concentrations are
28 sensitive to the primary $\text{PM}_{2.5}$ emissions, followed by NH_3 , and relatively insensitive to NO_x
29 and SO_2 . During August, gaseous precursors make larger contributions to $\text{PM}_{2.5}$
30 concentrations than primary $\text{PM}_{2.5}$, with similar contributions from NH_3 , SO_2 , and NO_x . We
31 also characterized the nonlinearity in the response of $\text{PM}_{2.5}$ to emission changes and
32 illustrated the underlying chemical processes. For example, the sensitivity of $\text{PM}_{2.5}$ to gaseous

1 precursors increases notably when more control efforts are taken, due to the transition
2 between NH₃-rich and NH₃-poor conditions. In January, the response of PM_{2.5} to NO_x
3 emissions is negative for relatively small reductions, but becomes positive for large
4 reductions.

5 The assessment of the response of PM_{2.5} and its inorganic components to precursor emissions
6 over the YRD region has important policy implications. First, the control of primary PM_{2.5}
7 emissions, especially those of the industrial and residential sources, should be enhanced
8 considering their large contribution to PM_{2.5} concentrations. Second, NO_x emissions need be
9 reduced substantially in order to mitigate the adverse effect on PM_{2.5} concentrations at
10 relatively small reduction ratio. Third, the control of NH₃ should be implemented in
11 heavy-pollution areas in winter due to its significant effect on PM_{2.5}. Fourth, it is essential to
12 implement region-dependent emission reduction targets based on the above-quantified
13 interactions among regions.

14 Except for identification of major emission sources, the ERSM technique has several other
15 practical applications. First, it allows us to calculate the required emission reductions to attain
16 a certain environmental target. Specifically, we alter the emission ratios of various control
17 variables and calculate the “real-time” response of PM_{2.5} concentrations with ERSM
18 repeatedly until the standard is attained. Second, ERSM can be applied to design optimal
19 control options, which could be determined through cost-effective optimization once ERSM is
20 coupled with control cost models/functions that links the emission reductions with private
21 costs.

22 The ERSM technique still has several limitations. Firstly, the technique currently does not
23 consider the variability of meteorological conditions. Secondly, although the ERSM technique
24 represents an essential improvement compared with the conventional RSM technique, it
25 usually needs over 500 emission scenarios for a medium-size problem. Future studies should
26 be done to further reduce the number of scenarios required while assuring the accuracy of the
27 response surfaces. Thirdly, the emission scenarios required to build the response surface
28 depends strictly on the experimental design (e.g., selection of geographical regions and
29 control variables). It is not necessary to recompute lots of CTM simulations if we make minor
30 revision on the experimental design. For example, if one more geographical area is added, we
31 just need to (1) add a parallel group of emission scenarios where the control variables of the
32 added geographical area change while those of the other regions remain the base-case levels,

1 and (2) recompute the emission scenarios where the control variables of all regions change
2 simultaneously. Another example, if the selected emission sectors in a specific geographical
3 area are changed, we just need to recompute the group of emission scenarios where the
4 control variables of this geographical area change while those of the other regions remain the
5 base-case levels. However, if the experimental design is significantly changed (e.g., change of
6 selected pollutants, or change of selected emission sectors in all regions), most of the CTM
7 simulations need to be recomputed. The users need to carefully design the experiment before
8 performing the CTM simulations.

11 **Code availability**

12 All codes needed to run ERSM v1.0 in MATLAB[®] are available upon the request. Any
13 potential user interested in the model should contact S. X. Wang, and any feedback on them is
14 welcome. Procedures to run the model and sources of external data files are properly
15 documented in a Manual.doc file.

17 **Author contribution**

18 B. Zhao, J. Xing, and S. X. Wang developed the underlying algorithms of the model. B. Zhao
19 and K. Fu developed the model code and performed the simulations. B. Zhao, K. Fu and W. J.
20 Wu conducted the model validation. B. Zhao and S. X. Wang prepared the manuscript with
21 contributions from all co-authors. J. S. Fu, C. Jang, Y. Zhu, X. Y. Dong, Y. Gao, J. D. Wang,
22 and J. M. Hao provided important academic guidance.

24 **Acknowledgment.** This work was sponsored by National Natural Science Foundation of
25 China (21221004), Strategic Priority Research Program of the Chinese Academy of Sciences
26 (XBD05020300), and MEP's Special Funds for Research on Public Welfares (201409002,
27 201309009). The authors also appreciate the support from Collaborative Innovation Center
28 for Regional Environmental Quality of Tsinghua University.

30 **References**

31 Amann, M., Cofala, J., Gzella, A., Heyes, C., Klimont, Z., and Schopp, W.: Estimating
32 concentrations of fine particulate matter in urban background air of European cities, Interim

1 Report IR-07-001, available at <http://www.iiasa.ac.at>, International Institute for Applied
2 Systems Analysis, Laxenburg, Austria, 50, 2007.

3 Carlton, A. G., Bhave, P. V., Napelenok, S. L., Edney, E. D., Sarwar, G., Pinder, R. W.,
4 Pouliot, G. A., and Houyoux, M.: Model Representation of Secondary Organic Aerosol in
5 CMAQv4.7, *Environ. Sci. Technol.*, 44, 8553-8560, DOI 10.1021/Es100636q, 2010.

6 Carmichael, G. R., Sandu, A., and Potra, F. A.: Sensitivity analysis for atmospheric chemistry
7 models via automatic differentiation, *Atmos. Environ.*, 31, 475-489, DOI
8 10.1016/S1352-2310(96)00168-9, 1997.

9 Dickerson, R. R., Stedman, D. H., and Delany, A. C.: Direct Measurements of Ozone and
10 Nitrogen-Dioxide Photolysis Rates in the Troposphere, *J. Geophys. Res-Oc. Atm.*, 87,
11 4933-4946, DOI 10.1029/Jc087ic07p04933, 1982.

12 Dong, X. Y., Li, J., Fu, J. S., Gao, Y., Huang, K., and Zhuang, G. S.: Inorganic aerosols
13 responses to emission changes in Yangtze River Delta, China, *Sci. Total. Environ.*, 481,
14 522-532, DOI 10.1016/j.scitotenv.2014.02.076, 2014.

15 Fu, J. S., Brill, E. D., and Ranjithan, S. R.: Conjunctive use of models to design cost-effective
16 ozone control strategies, *J. Air. Waste. Manage.*, 56, 800-809, 2006.

17 Fu, X., Wang, S. X., Zhao, B., Xing, J., Cheng, Z., Liu, H., and Hao, J. M.: Emission
18 inventory of primary pollutants and chemical speciation in 2010 for the Yangtze River
19 Delta region, China, *Atmos. Environ.*, 70, 39-50, DOI 10.1016/j.atmosenv.2012.12.034,
20 2013.

21 Guenther, A., Karl, T., Harley, P., Wiedinmyer, C., Palmer, P. I., and Geron, C.: Estimates of
22 global terrestrial isoprene emissions using MEGAN (Model of Emissions of Gases and
23 Aerosols from Nature), *Atmos. Chem. Phys.*, 6, 3181-3210, 2006.

24 Hakami, A., Odman, M. T., and Russell, A. G.: High-order, direct sensitivity analysis of
25 multidimensional air quality models, *Environ. Sci. Technol.*, 37, 2442-2452, DOI
26 10.1021/Es020677h, 2003.

27 Hakami, A., Seinfeld, J. H., Chai, T. F., Tang, Y. H., Carmichael, G. R., and Sandu, A.:
28 Adjoint sensitivity analysis of ozone nonattainment over the continental United States,
29 *Environ. Sci. Technol.*, 40, 3855-3864, DOI 10.1021/Es052135g, 2006.

30 Heyes, C., Schopp, W., Amann, M., and Unger, S.: A reduced-form model to predict
31 long-term ozone concentrations in Europe, Interim Report WP-96-12, available at
32 <http://www.iiasa.ac.at>, International Institute for Applied Systems Analysis, Laxenburg,
33 Austria, 58, 1996.

34 Hwang, J. T., Dougherty, E. P., Rabitz, S., and Rabitz, H.: Greens Function Method of
35 Sensitivity Analysis in Chemical-Kinetics, *J. Chem. Phys.*, 69, 5180-5191, DOI
36 10.1063/1.436465, 1978.

37 Iman, R. L., Davenport, J. M., and Zeigler, D. K.: Latin Hypercube Sampling (Program User's
38 Guide), Sandia National Laboratories, Albuquerque, NM, U.S. Technical Report
39 SAND79-1473, 78, 1980.

40 Milford, J. B., Russell, A. G., and Mcrae, G. J.: A New Approach to Photochemical
41 Pollution-Control - Implications of Spatial Patterns in Pollutant Responses to Reductions in
42 Nitrogen-Oxides and Reactive Organic Gas Emissions, *Environ. Sci. Technol.*, 23,
43 1290-1301, DOI 10.1021/Es00068a017, 1989.

44 Nel, A.: Air pollution-related illness: Effects of particles, *Science*, 308, 804-806, DOI
45 10.1126/science.1108752, 2005.

46 Robinson, A. L., Donahue, N. M., Shrivastava, M. K., Weitkamp, E. A., Sage, A. M.,
47 Grieshop, A. P., Lane, T. E., Pierce, J. R., and Pandis, S. N.: Rethinking organic aerosols:

1 Semivolatile emissions and photochemical aging, *Science*, 315, 1259-1262, DOI
2 10.1126/science.1133061, 2007.

3 Russell, A., Milford, J., Bergin, M. S., Mcbride, S., Mcnair, L., Yang, Y., Stockwell, W. R.,
4 and Croes, B.: Urban Ozone Control and Atmospheric Reactivity of Organic Gases,
5 *Science*, 269, 491-495, DOI 10.1126/science.269.5223.491, 1995.

6 Sandu, A., Daescu, D. N., Carmichael, G. R., and Chai, T. F.: Adjoint sensitivity analysis of
7 regional air quality models, *J. Comput. Phys.*, 204, 222-252, DOI
8 10.1016/j.jcp.2004.10.011, 2005.

9 Sandu, A., and Zhang, L.: Discrete second order adjoints in atmospheric chemical transport
10 modeling, *J. Comput. Phys.*, 227, 5949-5983, DOI 10.1016/j.jcp.2008.02.011, 2008.

11 Santner, T. J., Williams, B. J., and Notz, W.: *The Design and Analysis of Computer*
12 *Experiments*, Springer Verlag, New York, U.S., 283 pp., 2003.

13 Simon, H., Baker, K. R., Akhtar, F., Napelenok, S. L., Possiel, N., Wells, B., and Timin, B.:
14 A Direct Sensitivity Approach to Predict Hourly Ozone Resulting from Compliance with
15 the National Ambient Air Quality Standard, *Environ. Sci. Technol.*, 47, 2304-2313, DOI
16 10.1021/Es303674e, 2013.

17 Stocker, T. F., Qin, D., Plattner, G.-K., Tignor, M., Allen, S. K., Boschung, J., Nauels, A., Xia,
18 Y., Bex, V., and Midgley, P. M.: *Climate Change 2013: The Physical Science Basis.*
19 *Contribution of Working Group I to the Fifth Assessment Report of the Intergovernmental*
20 *Panel on Climate Change*, Cambridge University Press, Cambridge, United Kingdom and
21 New York, NY, USA, 1535 pp., 2013.

22 U.S. Environmental Protection Agency: Technical support document for the proposed PM
23 NAAQS rule: Response Surface Modeling, Office of Air Quality Planning and Standards,
24 U.S. Environmental Protection Agency, Research Triangle Park, NC, U.S., 48, 2006a.

25 U.S. Environmental Protection Agency: Technical support document for the proposed mobile
26 source air toxics rule: ozone modeling, Office of Air Quality Planning and Standards, U.S.
27 Environmental Protection Agency, Research Triangle Park, NC, U.S., 49, 2006b.

28 Wang, L. H., and Milford, J. B.: Reliability of optimal control strategies for photochemical air
29 pollution, *Environ. Sci. Technol.*, 35, 1173-1180, DOI 10.1021/Es001358y, 2001.

30 Wang, S. X., Xing, J., Jang, C. R., Zhu, Y., Fu, J. S., and Hao, J. M.: Impact assessment of
31 ammonia emissions on inorganic aerosols in east China using response surface modeling
32 technique, *Environ. Sci. Technol.*, 45, 9293-9300, DOI 10.1021/Es2022347, 2011.

33 Wang, S. X., and Hao, J. M.: Air quality management in China: Issues, challenges, and
34 options, *J. Environ. Sci-China.*, 24, 2-13, DOI 10.1016/S1001-0742(11)60724-9, 2012.

35 Wang, S. X., Zhao, B., Cai, S. Y., Klimont, Z., Nielsen, C., McElroy, M. B., Morikawa, T.,
36 Woo, J. H., Kim, Y., Fu, X., Xu, J. Y., Hao, J. M., and He, K. B.: Emission trends and
37 mitigation options for air pollutants in East Asia, *Atmos. Chem. Phys. Discuss.*, 14,
38 2601-2674, DOI 10.5194/acpd-14-2601-2014, 2014.

39 Xing, J.: Study on the nonlinear responses of air quality to primary pollutant emissions,
40 Doctor thesis, School of Environment, Tsinghua University, Beijing, China, 138 pp., 2011
41 (in Chinese).

42 Xing, J., Wang, S. X., Jang, C., Zhu, Y., and Hao, J. M.: Nonlinear response of ozone to
43 precursor emission changes in China: a modeling study using response surface
44 methodology, *Atmos. Chem. Phys.*, 11, 5027-5044, DOI 10.5194/acp-11-5027-2011, 2011.

45 Yang, Y. J., Wilkinson, J. G., and Russell, A. G.: Fast, direct sensitivity analysis of
46 multidimensional photochemical models, *Environ. Sci. Technol.*, 31, 2859-2868, DOI
47 10.1021/Es970117w, 1997.

1 Yarwood, G., Emery, C., Jung, J., Nopmongcol, U., and Sakulyanontvittaya, T.: A method to
2 represent ozone response to large changes in precursor emissions using high-order
3 sensitivity analysis in photochemical models, *Geosci. Model. Dev.*, 6, 1601-1608, DOI
4 10.5194/gmd-6-1601-2013, 2013.

5 Zhang, Q., Streets, D. G., Carmichael, G. R., He, K. B., Huo, H., Kannari, A., Klimont, Z.,
6 Park, I. S., Reddy, S., Fu, J. S., Chen, D., Duan, L., Lei, Y., Wang, L. T., and Yao, Z. L.:
7 Asian emissions in 2006 for the NASA INTEX-B mission, *Atmos. Chem. Phys.*, 9,
8 5131-5153, 2009a.

9 Zhang, X. Y., Wang, Y. Q., Niu, T., Zhang, X. C., Gong, S. L., Zhang, Y. M., and Sun, J. Y.:
10 Atmospheric aerosol compositions in China: spatial/temporal variability, chemical
11 signature, regional haze distribution and comparisons with global aerosols, *Atmos. Chem.*
12 *Phys.*, 12, 779-799, DOI 10.5194/acp-12-779-2012, 2012.

13 Zhang, Y., Wen, X. Y., Wang, K., Vijayaraghavan, K., and Jacobson, M. Z.: Probing into
14 regional O₃ and particulate matter pollution in the United States: 2. An examination of
15 formation mechanisms through a process analysis technique and sensitivity study, *J.*
16 *Geophys. Res-Atmos.*, 114, DOI 10.1029/2009jd011900, 2009b.

17 Zhao, B., Wang, S. X., Dong, X. Y., Wang, J. D., Duan, L., Fu, X., Hao, J. M., and Fu, J.:
18 Environmental effects of the recent emission changes in China: implications for particulate
19 matter pollution and soil acidification, *Environ. Res. Lett.*, 8, DOI
20 10.1088/1748-9326/8/2/024031, 2013a.

21 Zhao, B., Wang, S. X., Liu, H., Xu, J. Y., Fu, K., Klimont, Z., Hao, J. M., He, K. B., Cofala,
22 J., and Amann, M.: NO_x emissions in China: historical trends and future perspectives,
23 *Atmos. Chem. Phys.*, 13, 9869-9897, DOI 10.5194/acp-13-9869-2013, 2013b.

24 Zhao, B., Wang, S. X., Wang, J. D., Fu, J. S., Liu, T. H., Xu, J. Y., Fu, X., and Hao, J. M.:
25 Impact of national NO_x and SO₂ control policies on particulate matter pollution in China,
26 *Atmos. Environ.*, 77, 453-463, DOI 10.1016/j.atmosenv.2013.05.012, 2013c.

27
28

1 Tables and figures

2 Table 1. Description of the RSM/ERSM prediction systems developed in this study.

method	variable number	control variables	scenario number	scenario details
conventional RSM technique	5	total emissions of NO _x , SO ₂ , NH ₃ , NMVOC, and PM _{2.5}	101	1 CMAQ base case; 100 ^a scenarios generated by applying LHS method for the 5 variables.
ERSM technique	36	9 variables in each of the 4 regions, including 6 gaseous variables, i.e., (1) NO _x /Power plants (2) NO _x /Industrial and residential (3) NO _x /Transportation (4) SO ₂ /Power plants (5) SO ₂ /Industrial and Residential (6) NH ₃ /All sectors, and 3 primary PM _{2.5} variables, i.e., (7) PM _{2.5} /Power plants (8) PM _{2.5} /Industrial and residential (9) PM _{2.5} /Transportation.	663	1 CMAQ base case; 600 scenarios, including 150 ^a scenarios generated by applying LHS method for the gaseous control variables in Shanghai, 150 scenarios generated in the same way for Jiangsu, 150 scenarios for Zhejiang, 150 scenarios for Others; 50 ^a scenarios generated by applying LHS method for the total NO _x , SO ₂ , and NH ₃ emissions; 12 scenarios where one primary PM _{2.5} control variable is set to 0.25 for each scenario.

3 ^a 100, 150 and 50 scenarios are needed for the response surfaces for 5, 6 and 3 variables, respectively (Xing et
4 al., 2011; Wang et al., 2011).

5

6 Table 2. Comparison of PM_{2.5} concentrations predicted by the ERSM technique with
7 out-of-sample CMAQ simulations.

	January			August		
	Shanghai	Jiangsu	Zhejiang	Shanghai	Jiangsu	Zhejiang
Correlation coefficient	0.989	0.980	0.987	0.995	0.997	0.994
Mean Normalized Error (MNE)	1.0%	0.7%	0.9%	0.8%	0.5%	1.7%
Maximum Normalized Error (NE)	4.5%	3.0%	5.2%	10.2%	7.7%	9.6%
95% percentile of NEs	2.8%	2.7%	3.5%	3.0%	1.6%	3.1%
MNE (case 33-36)	0.0%	0.0%	0.0%	0.1%	0.1%	0.1%
Maximum NE (case 33-36)	0.1%	0.1%	0.1%	0.1%	0.1%	0.2%

8

1

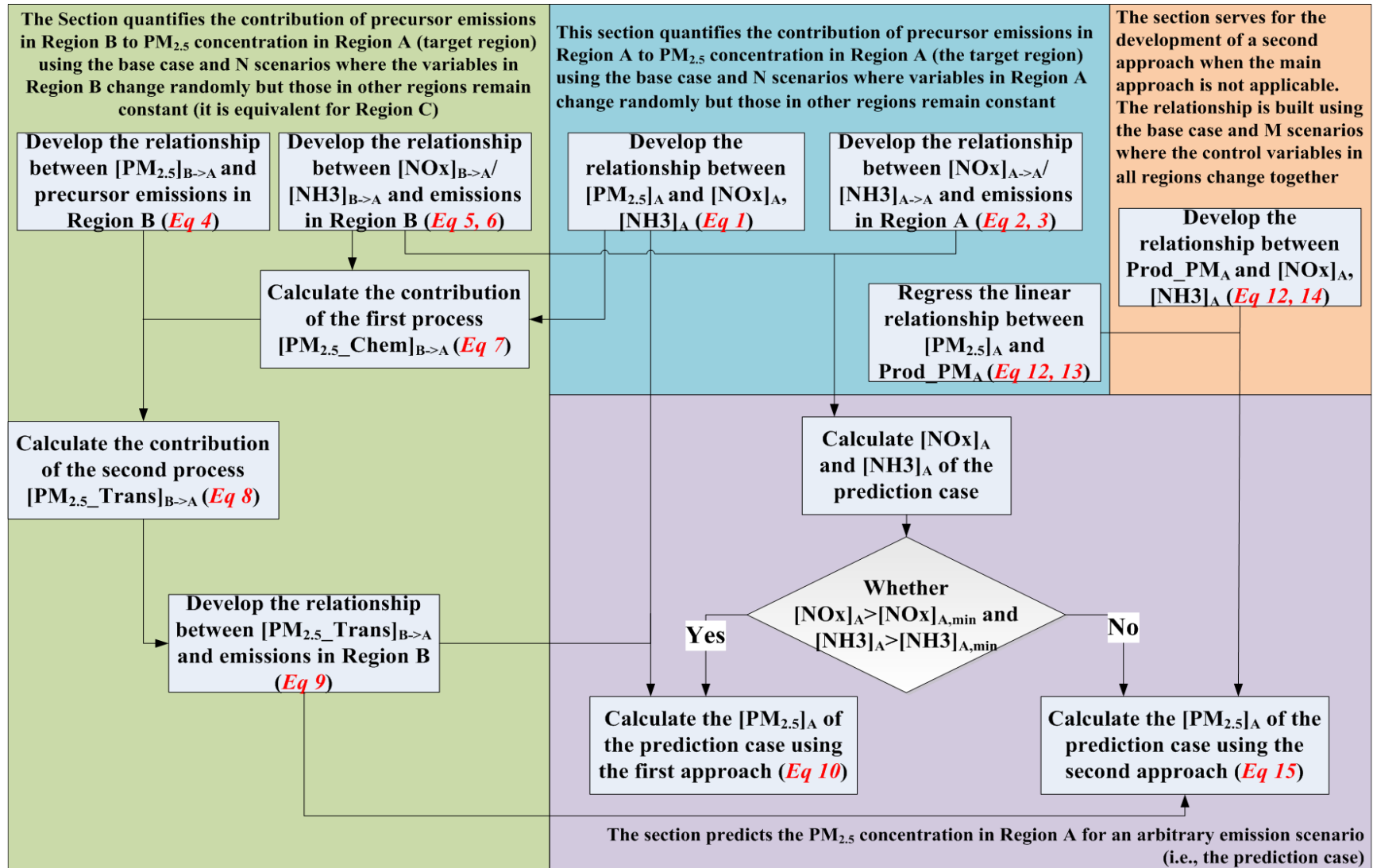
2 Table 3. Contribution of primary PM_{2.5} and gaseous precursor (NO_x, SO₂, NH₃) emissions

3 from individual regions to PM_{2.5} concentrations.

	January			August		
	Shanghai	Jiangsu	Zhejiang	Shanghai	Jiangsu	Zhejiang
Emissions of Primary PM _{2.5} in Shanghai	35.5%	1.1%	1.3%	36.9%	1.0%	0.4%
Emissions of Primary PM _{2.5} in Jiangsu	5.6%	35.0%	4.1%	2.2%	37.5%	0.9%
Emissions of Primary PM _{2.5} in Zhejiang	1.9%	2.3%	32.2%	4.3%	2.5%	42.8%
Emissions of Primary PM _{2.5} in Others	2.9%	2.9%	1.7%	2.0%	1.9%	1.5%
Emissions of Primary PM _{2.5} in four regions	46.0%	41.2%	39.4%	45.4%	42.9%	45.7%
Emissions of NO _x , SO ₂ , and NH ₃ in Shanghai	11.3%	0.2%	1.0%	18.9%	1.8%	2.5%
Emissions of NO _x , SO ₂ , and NH ₃ in Jiangsu	3.3%	11.7%	3.9%	5.2%	30.1%	4.3%
Emissions of NO _x , SO ₂ , and NH ₃ in Zhejiang	2.7%	4.3%	20.9%	18.3%	12.6%	36.3%
Emissions of NO _x , SO ₂ , and NH ₃ in Others	1.7%	2.4%	2.8%	5.7%	4.6%	7.2%
Emissions of NO _x , SO ₂ , and NH ₃ in four regions	25.2%	24.9%	35.7%	48.3%	50.4%	47.7%
Emissions of Primary PM _{2.5} in the outer domain	7.4%	9.1%	6.3%	0.7%	0.8%	1.6%
Emissions of NO _x , SO ₂ , and NH ₃ in outer domain	20.6%	24.5%	19.1%	6.6%	7.1%	6.1%

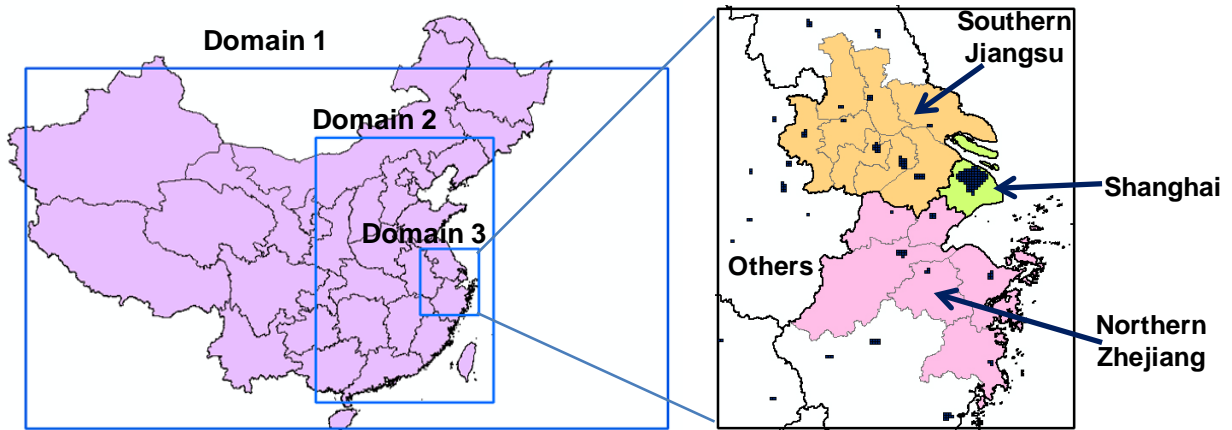
4

5



1
 2 Figure 1. A flowchart illustrating the ERSM technique using the simplified case described in Sect. 2.1. Different background colors
 3 represent the procedures conducted using different groups of emission scenarios, as indicated on the top/bottom of the colored areas.

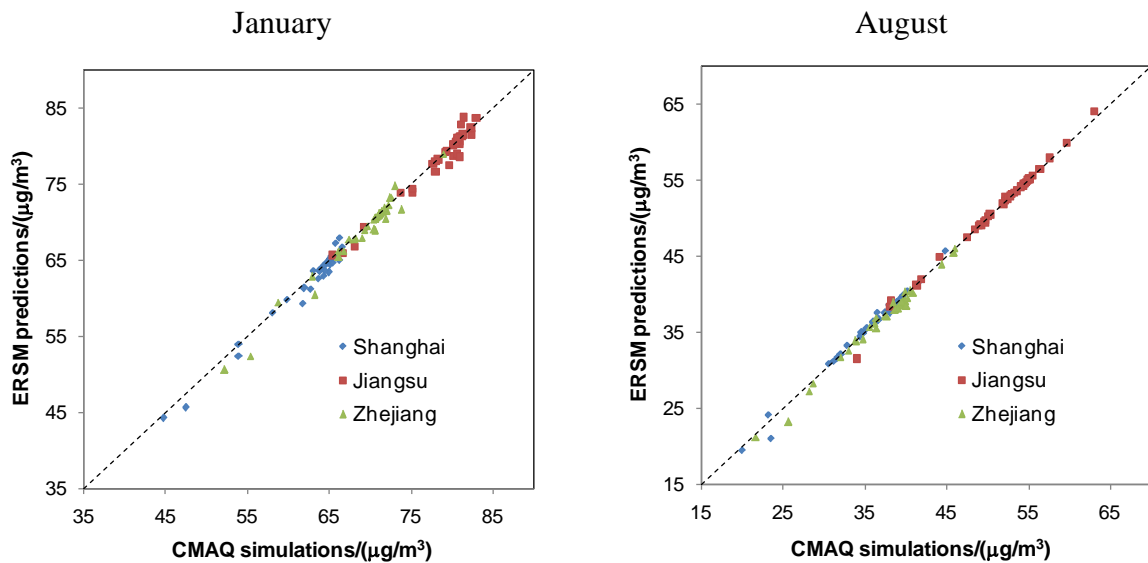
1



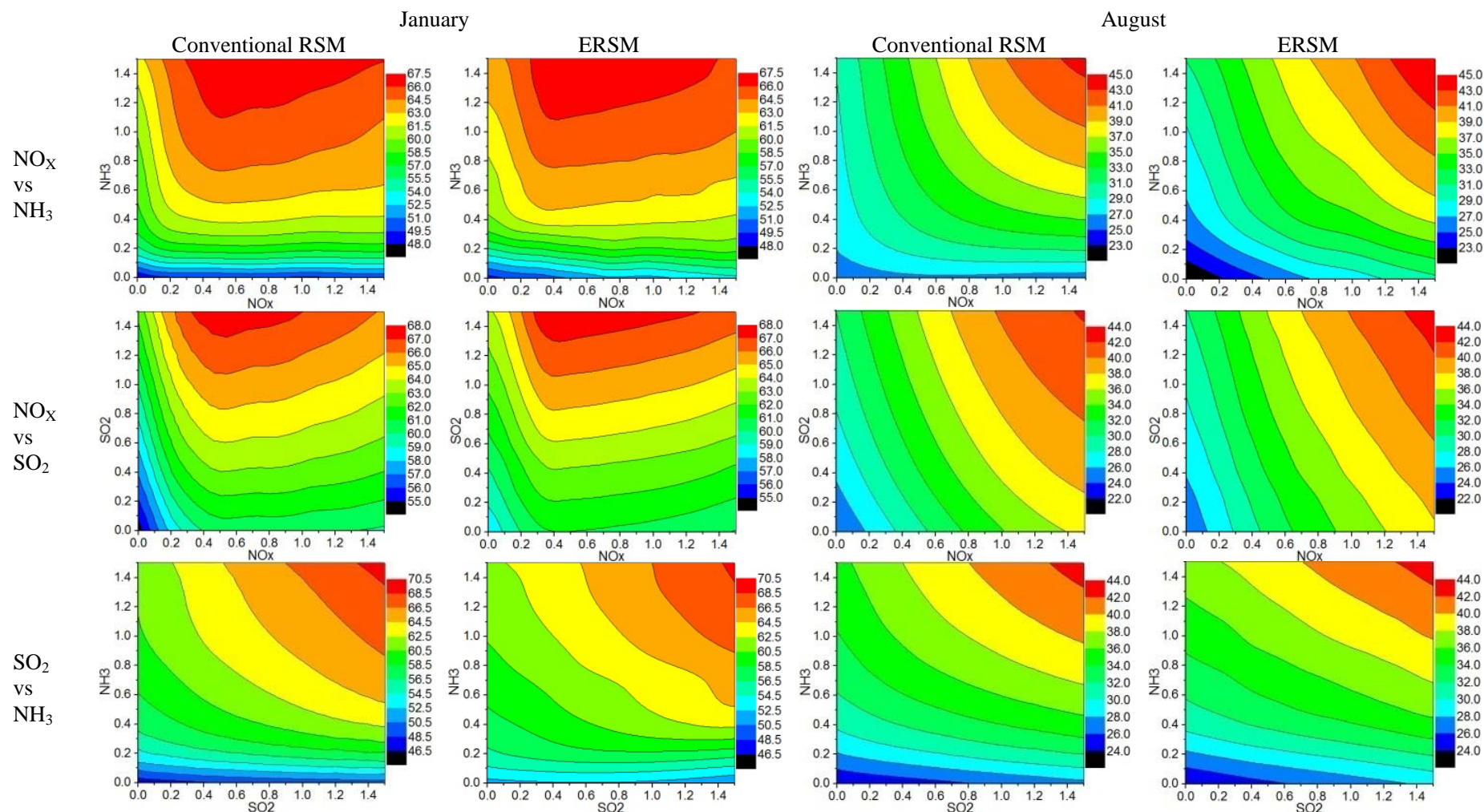
2

3 Figure 2. Triple nesting domains used in CMAQ simulation (left) and the definition of four
4 regions in the innermost domain, denoted by different colors (right). The black lines in the left
5 figure represent provincial boundaries; the thick black lines and the thin grey lines in the right
6 figure represent the provincial boundaries and city boundaries, respectively. The dark blue
7 grids in the right figure represent the urban areas of major cities.

8

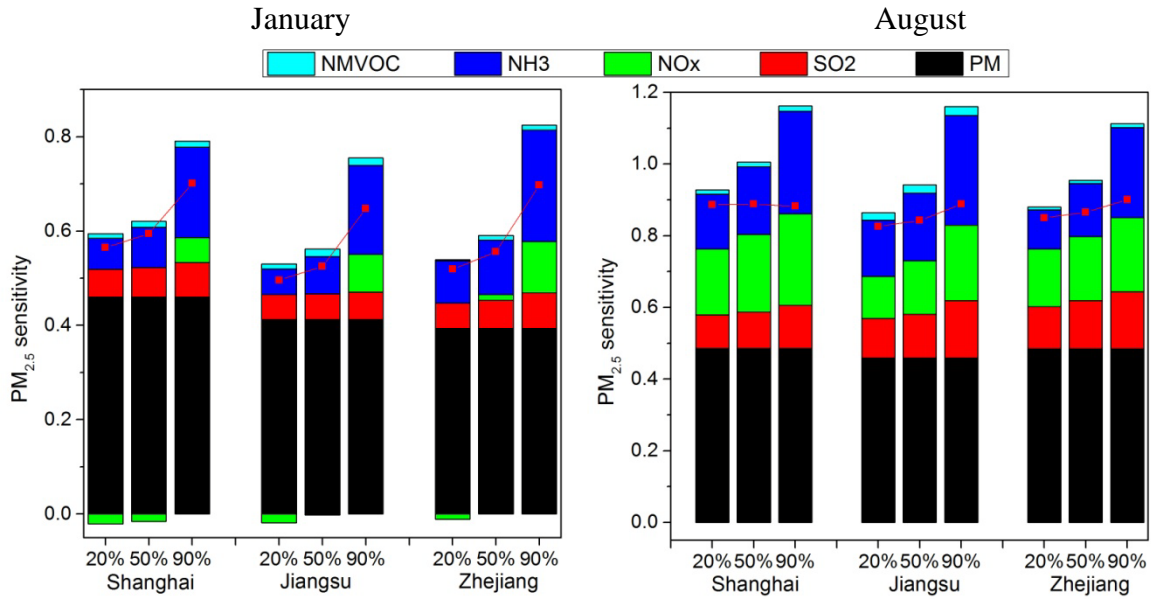


9 Figure 3. Comparison of $PM_{2.5}$ concentrations predicted by the ERSM technique with
10 out-of-sample CMAQ simulations. The dashed line is the one-to-one line indicating perfect
11 agreement.

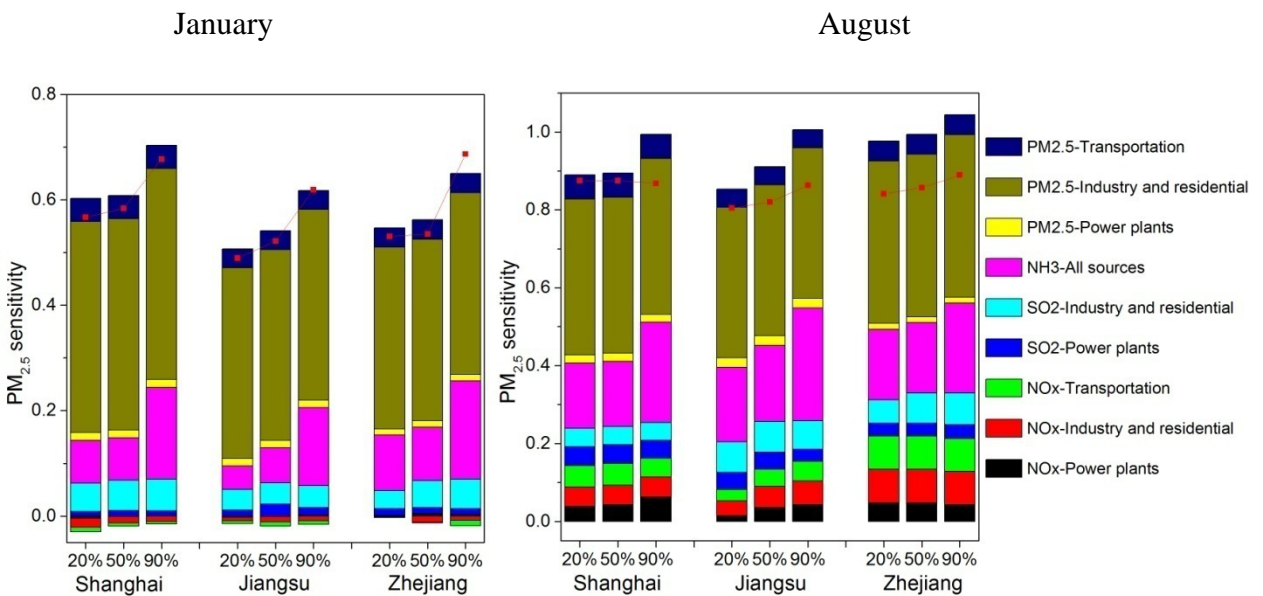


1 Figure 4. Comparison of the 2-D isopleths of $PM_{2.5}$ concentrations in Shanghai in response to the simultaneous changes of precursor
 2 emissions in all regions derived from the conventional RSM technique and the ERSM technique. The X- and Y-axis shows the emission
 3 ratio, defined as the ratios of the changed emissions to the emissions in the base case. The different colors represent different $PM_{2.5}$
 4 concentrations (unit: $\mu g m^{-3}$).

1

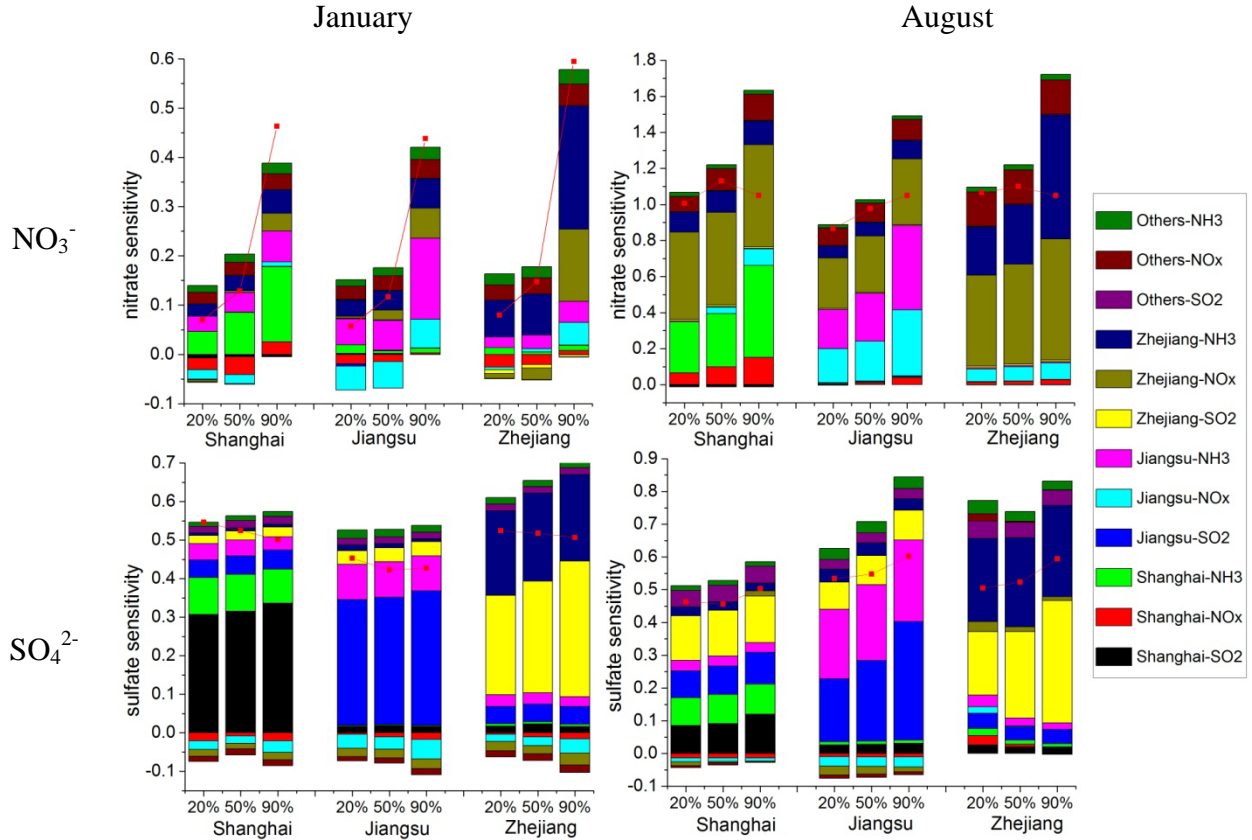


2 Figure 5. Sensitivity of $PM_{2.5}$ concentrations to the stepped control of individual air pollutants.
 3 The X-axis shows the reduction ratio ($= 1 - \text{emission ratio}$). The Y-axis shows $PM_{2.5}$
 4 sensitivity, which is defined as the change ratio of concentration divided by the reduction
 5 ratio of emissions. The colored bars denote the $PM_{2.5}$ sensitivities when a particular pollutant
 6 is controlled while the others stay the same as the base case; the red dotted line denotes the
 7 $PM_{2.5}$ sensitivity when all emission sources are controlled simultaneously.
 8



9 Figure 6. Sensitivity of $PM_{2.5}$ concentrations to the stepped control of individual air pollutants
 10 from individual sectors. The X-axis shows the reduction ratio ($= 1 - \text{emission ratio}$). The
 11 Y-axis shows $PM_{2.5}$ sensitivity, which is defined as the change ratio of concentration divided
 12 by the reduction ratio of emissions. The colored bars denote the $PM_{2.5}$ sensitivities when a

1 particular emission source is controlled while the others stay the same as the base case; the
 2 red dotted line denotes the $PM_{2.5}$ sensitivity when all emission sources are controlled
 3 simultaneously.
 4



5 Figure 7. Sensitivity of NO_3^- and SO_4^{2-} concentrations to the stepped control of individual air
 6 pollutants in individual regions. The X-axis shows the reduction ratio (= 1 – emission ratio).
 7 The Y-axis shows NO_3^-/SO_4^{2-} sensitivity, which is defined as the change ratio of NO_3^-/SO_4^{2-}
 8 concentration divided by the reduction ratio of emissions. The colored bars denote the
 9 NO_3^-/SO_4^{2-} sensitivities when a particular emission source is controlled while the others stay
 10 the same as the base case; the red dotted line denotes the NO_3^-/SO_4^{2-} sensitivity when all
 11 emission sources are controlled simultaneously.